Can the inhibition of cytochrome P450 in aquatic invertebrates due to azole fungicides be estimated with in silico and in vitro models and extrapolated between species?

Gottardi, Michele; Tyzack, Jonathan D.; Bender, Andreas; Cedergreen, Nina

Published in:
Aquatic Toxicology

DOI:
10.1016/j.aquatox.2018.05.017

Publication date:
2018

Document version
Early version, also known as pre-print

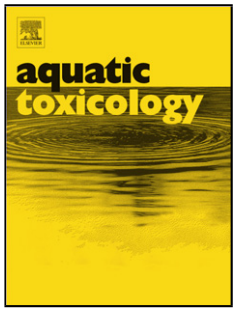

Title: Can the inhibition of cytochrome P450 in aquatic invertebrates due to azole fungicides be estimated with *in silico* and *in vitro* models and extrapolated between species?

Authors: Michele Gottardi, Jonathan D. Tyzack, Andreas Bender, Nina Cedergreen

PII: S0166-445X(18)30250-9
DOI: https://doi.org/10.1016/j.aquatox.2018.05.017
Reference: AQTOX 4946

To appear in: *Aquatic Toxicology*

Received date: 12-3-2018
Revised date: 23-5-2018
Accepted date: 24-5-2018

Please cite this article as: Gottardi M, Tyzack JD, Bender A, Cedergreen N, Can the inhibition of cytochrome P450 in aquatic invertebrates due to azole fungicides be estimated with *in silico* and *in vitro* models and extrapolated between species?, *Aquatic Toxicology* (2018), https://doi.org/10.1016/j.aquatox.2018.05.017

Can the inhibition of cytochrome P450 in aquatic invertebrates due to azole fungicides be estimated with *in silico* and *in vitro* models and extrapolated between species?

Michele Gottardi[a], *Jonathan D. Tyzack*[b], *Andreas Bender*[c], *Nina Cedergreen*[a,*]

[a]Department of Plant and Environmental Sciences, University of Copenhagen, Thorvaldsensvej 40, 1871 Frederiksberg, Denmark

[b]EMBL-EBI, Wellcome Genome Campus, Hinxton, Cambridgeshire, CB10 1SD, United Kingdom

[c]Centre for Molecular Informatics, Department of Chemistry, University of Cambridge, Lensfield Road, Cambridge, CB2 1EW, United Kingdom

[*]Corresponding author, Department of Plant and Environmental Sciences, University of Copenhagen, Thorvaldsensvej 40, 1871 Frederiksberg, Denmark, email: ncf@plen.ku.dk

Highlights

- The inhibition of cytochrome P450 due to azole fungicides can be estimated in vitro and to a lesser extent in silico for the insect larva C. riparius but not for the snail L. stagnalis.
- Organisms may present very different enzymatic susceptibility toward azole inhibition, making species-species extrapolation not straightforward

ABSTRACT

Azole fungicides, designed to halt fungal growth by specific inhibition of fungal cytochrome P450 (CYP51), inhibit cytochrome P450s involved in the metabolism of xenobiotics in several non-target organisms thus raising environmental concern. The present study investigates the degree by which inhibition strengths of azoles toward cytochrome P450 in rat liver, the insect *Chironomus riparius* larvae and the snail *Lymnaea stagnalis* can be extrapolated from estimated *in silico* affinities. Azoles' affinities toward human cytochrome P450 isoforms involved in xenobiotic metabolism (CYP3A4, CYP2C9 and CYP2D6) as well as fungal CYP51 were estimated with a ligand-protein docking model based on the ChemScore scoring function. Estimated affinities toward the selected enzymatic structures correlated strongly with measured inhibition strengths in rat liver (ChemScore vs. $\log IC_{50}$ among cytochrome P450 isoforms: $-0.662 < r < -0.891$, $n = 17$ azoles), while weaker correlations were found for *C. riparius* larvae ($-0.167 < r < -0.733$, $n = 9$) and *L. stagnalis* ($-0.084 < r < -0.648$, $n = 8$). Inhibition strengths toward *C. riparius* and rat liver activities were found to be highly correlated to each other (r: 0.857) while no significant relationship was found between either of the species and *L. stagnalis*. The inhibition of cytochrome P450 due to azole fungicides could be estimated *in vitro* and to a lesser extent *in silico* for *C. riparius* but not for *L. stagnalis*, possibly due to different enzymatic susceptibility toward azole inhibition among the species.

ABBREVIATIONS

ACN, acetonitrile; BSA, bovine serum albumin; DTT, DL-dithiothreitol; ECOD, 7-ethoxycoumarin-O-dealkylase; EDTA, ethylenediaminetetraacetic acid disodium salt dihydrate; IC_{50}, half maximal inhibitory concentration; K_2HPO_4 $3H_2O$, potassium phosphate dibasic trihydrate; KH_2PO_4, potassium dihydrogen phosphate; MFO Mixed function oxidase; NADPH, ß-nicotinamide adenine dinucleotide-phosphate reduced tetrasodium salt hydrate; PMSF, phenylmethanesulfonyl fluoride

KEYWORDS

Enzymatic assay, aquatic invertebrate, azole fungicide, in silico model, in vitro model

1 Introduction

Azole fungicides are a group of plant protection agents extensively use in agriculture, accounting for approximately 25 % of the total production of fungicides worldwide.[1] Furthermore, they are also used as antifungal drugs in humans as well as in livestock.[2] Azole fungicides can enter surface water due to spray drift and run-off after rain events,[3, 4] or through effluents of waste water treatment plants.[2] Azoles have been measured in surface water in concentrations usually ranging from 0.01 µg/L to 1 µg/L with peak concentrations of up to 175 µg/L.[5]

Azoles were designed to inhibit the fungal cytochrome P450 responsible for ergosterol biosynthesis (CYP51, lanosterol-14 α-demethylase). Ergosterol plays an important role in the

function and integrity of fungal membrane, hence, inhibition of its synthesis halts fungal growth.[6] The molecular structure of azoles is characterized by the presence of an azole ring, which contains either two (imidazoles) or three (triazoles) nitrogen atoms, resulting in different antifungal selectivity.[7] However, in addition to the target cytochrome P450 of fungi, azoles have also been shown to inhibit cytochrome P450s involved in detoxification in non-target organisms.[8-10] Inhibition of cytochrome P450 dependent detoxification is believed to be the main mechanism responsible for the ability of azoles to synergize the toxicity of other pesticides such as pyrethroid insecticides.[8, 11] Under certain conditions, cytochrome P450s responsible for detoxification may also be induced thereby synergizing the toxicity of compounds that require activation by cytochrome P450 dependent oxidations to exert their toxic effect, such as certain organophosphate insecticides.[12] Induction of cytochrome P450s is, however, not specifically related to azoles, but a more general property of several groups of xenobiotics,[11] and it will therefore not be discussed further in the present study.

Azoles reversibly inhibit cytochrome P450s by coordination of the azole ring to the heme-iron as well as through molecular interaction with the enzyme's hydrophobic regions.[13] In general, the inhibitory strength of azole fungicides toward cytochrome P450s is believed to be governed by several factors, namely the affinity of the nitrogen electron lone pair of the azole ring to the heme-iron and the presence of substituents that may sterically modify this affinity, the hydrophobicity of the overall molecule (which is generally favorable for binding, given the hydrophobicity of the enzyme active cavity) and the complementarity between inhibitor geometry and enzyme active site.[13]

A large suite of cytochrome P450s exists within the same organism, not only catalyzing xenobiotics but also a range of endogenous processes, of which those governing endocrine

hormone regulations have received the most attention.[14-16] Cytochrome P450s involved in xenobiotic detoxification are membrane bound proteins primarily present in the endoplasmic reticulum (microsomal fraction) which mainly catalyze oxidation reactions.[17, 18] Cytochrome P450s involved in detoxification generally lack the substrate specificity of cytochrome P450s involved in the metabolism of endogenous molecules. Different cytochrome P450s involved in detoxification have been shown to metabolize similar substrates and similar cytochrome P450s can metabolize different substrates.[14-16] In the present study, the characterization of cytochrome P450 activity relevant for detoxification and its inhibition in different species is based on the ability of the extracted microsomal fraction to metabolize the same standard substrate, 7-ethoxycoumarin.[19]

Knowledge of inhibition strength of azole fungicides in relevant aquatic species would provide a tool to better understand and assess the ecotoxicological impact of these chemicals. Among the relevant aquatic species, the present study focuses on aquatic invertebrates, which are currently employed as test organisms for ecotoxicological studies and therefore form the basis of aquatic risk assessment of chemicals. Extraction of microsomal material and measurements of cytochrome P450 activities in small aquatic invertebrates used in ecotoxicological studies have been shown to be time consuming and sometimes not possible to carry out with current techniques. This is because organs rich in cytochrome P450s cannot be dissected out of very small organisms, and because homogenization of the whole organisms can release endogenous substances that attenuate *in vitro* enzymatic activity (Gottardi, et al. [20] and references therein). Therefore, the prediction of inhibition strengths, by using computer based approaches and/or by measurements on commercially available enzymatic materials extracted from other species,

could provide a quick and cheap screening tool to identify strong cytochrome P450 inhibitors and subsequently potential synergistic substances in environmental chemical mixtures.

Ligand-protein docking is a well-established computer based (*in silico*) method that predicts the orientations of small organic molecules (ligands) in protein binding pockets[21, 22] as well as their binding affinities in the form of docking scores.[22] The method, although not free from limitations,[21, 22] has been recently used to investigate inhibition of aromatase (cytochrome P450 CYP19 involved in steroidogenesis) by azole fungicides, obtaining good degrees of correlation between docking scores and experimentally measured inhibition strengths of azoles toward aromatase activity in human (r: -0.81), fish brain (r: -0.69) and fish ovaries (r: -0.85).[1] However, the use of this approach for ecotoxicologically relevant aquatic invertebrates presents additional limitations, since the specific types and roles of cytochrome P450 present in these organisms are generally unknown. Therefore, crystallized cytochrome P450 structures are currently not available and since gene sequencing of non-target invertebrates is only in its infancy, also the creation of cytochrome P450 structures from homology models is limited.[23] At present, *in silico* investigations of chemical interactions with cytochrome P450s in aquatic invertebrates must therefore rely on the available (mainly human) cytochrome P450 crystallized structures.

The use of models based on cytochrome P450 structures obtained from different organisms may nonetheless be possible. The overall three-dimensional structure of cytochrome P450s and the site responsible for the catalytic activity (heme-group) are conserved in practically all organisms where cytochrome P450s are found,[18, 24] whereas the position of structural elements in the active cavity accounts for substrate and/or inhibitor (un)specificity among the different isoforms.[18, 24] Therefore, inter species extrapolations of inhibition strengths may also be feasible for cytochrome P450s responsible for detoxification, as this group of enzymes is expected to

present substrate unspecificity and possibly to be conserved across species potentially exposed to the myriad of natural and artificial xenobiotics present in the environment.

The aim of the present study was to investigate the degree by which an *in silico* ligand-protein docking model, based on available human and fungal cytochrome P450 crystallized structures, could estimate experimentally measured inhibition strengths of selected azole fungicides (Table 1) toward microsomal cytochrome P450 activities of rat liver, insect *Chironomus riparius* larvae and snail *Lymnaea stagnalis*. Rat liver microsomes were chosen as a commercially available source of enzymatic material, widely used for *in vitro* cytochrome P450 activity assays. The non-target invertebrates *C. riparius* and *L. stagnalis* were chosen as model organisms representing insects and molluscs, respectively. Both species are widely present in the environment and are currently used as standard organisms for ecotoxicological studies.[25, 26] In addition, measurable cytochrome P450 activity of *C. riparius* has been shown to be inhibited by a range of azole fungicides in a previous investigation.[20]

The present study tested the following hypotheses: 1) *in silico* estimated affinities (docking scores) between azoles and different cytochrome P450 isoforms are strongly correlated to one another; 2) the estimated affinities, based solely on the azoles' molecular structures and the available crystallized cytochrome P450 structures, can be used to rank the inhibition strength of the azoles equally well in different species and 3) experimentally measured inhibition strengths of azole fungicides toward microsomal cytochrome P450 activities can be extrapolated between species from different phyla.

2 Materials and Methods

2.1 Azole fungicides and cytochrome P450 structures

Five imidazoles and 13 triazoles were selected based on their use in agriculture or medicine (Table 1, Figure S1). Their 3D structures were downloaded from the PubChem[27] or ZINC[28] databases in Structure Data File (.sdf) format or Sybyl Mol2 (.mol2) format.

A relatively large number of cytochrome P450 crystallized structures are available in The Protein Data Bank (PDB).[29] Among those, the structures of three human cytochrome P450 isoforms involved in xenobiotic detoxification were selected: CYP3A4, CYP2C9 and CYP2D6. Two crystallized structures were selected for each isoform, with or without the presence of a co-crystallized inhibitor. This was done to investigate whether the choice of a specific isoform, or a structure co-crystallized with an inhibitor, had an effect on the correlations between the docking scores and the experimentally measured inhibition strengths of the azoles. CYP3A4 was selected due to its highest abundance in human liver,[30] for which structures PDB 1TQN[31] (due to its use by Tyzack, et al. [32]) and 2V0M[33] (co-crystallized with the inhibitor ketoconazole, PDB ID: KLN, Figure S2) were selected. CYP2C9 is reported to be the second highest abundant cytochrome P450 in human liver,[30] for which structures PDB 1R9O[34] (due to best resolution and previous use by Tyzack, et al. [32]) and 4NZ2[35] (the newest structure available and co-crystallized with the inhibitor (2R)-N-[4-[(3-bromophenyl)sulfonyl]-2-chlorophenyl]- 3,3,3-trifluoro-2-hydroxy-2-methylpropanamide, PDB ID: 2QJ, Figure S2) were selected. CYP2D6 was selected due to its involvement in the oxidation of approximately 25% of pharmaceutical drugs oxidized by cytochrome P450s,[30] for which structures PDB 2F9Q,[33] (due to previous use by Tyzack, et al. [32]) and 4XRZ,[36] (the newest structure available and co-crystallized with the inhibitor (4aR,6R,8aS)-8a-(2,4-difluorophenyl)-6-(1H- pyrazol-4-yl)-4,4a,5,6,8,8a-hexahydropyrano[3,4- d][1,3]thiazin-2-amine, PDB ID: SI6, Figure S2) were selected. Additionally, the fungal cytochrome P450 isoform CYP51 was recently co-crystallized with several azole fungicides,[37] of which structure

PDB 5EAB (co-crystallized with the inhibitor tebuconazole, PDB ID: TBX, Figure S2) was selected.

2.2 Docking

Prior to docking, the 3D structures of all azole stereoisomers were prepared with the LigPrep module in Maestro, v. 2014-2[38] by addition of hydrogen atoms and energy minimization of molecular geometries (bond lengths and angles). The selected cytochrome P450 structures were prepared with the built-in wizard of GOLD 5.4[39, 40] by addition of hydrogens and removal of co-crystallized nonstandard residues (inhibitors, cofactors, ions, solvent and water molecules) if present.[41]

Among the available scoring functions available in GOLD 5.4[39, 40], the ChemScore function was selected due to its parametrization with measured binding affinities[42, 43] and available cytochrome P450 specific parameters[44] as well as the ability to deconstruct binding energies in terms of different contributions, which are directly related to the factors governing the inhibitory strength of azole fungicides toward cytochrome P450s. The ChemScore function estimates the total free energy change ($\Delta G_{binding}$) that results from ligand binding due to hydrogen bonds (ΔG_{hbond}), metal bonds (ΔG_{metal}), lipophilic interactions (ΔG_{lipo}) and non-rotatable ligand bonds (ΔG_{rot}) (Equation 1) with the addition of penalties based on clashes due to close molecular contacts (DE_{clash}), on internal torsion caused by poor internal conformation (DE_{int}) and on user implemented constrains (DE_{con}) (dimensionless unit, Equation 2).

$$\Delta G_{binding} = \Delta G_0 + \Delta G_{hbond} + \Delta G_{metal} + \Delta G_{lipo} + \Delta G_{rot} \quad \textbf{Equation 1}$$

Where ΔG_0 = -5.48, ΔG_{hbond} = -3.34 * S_{hbond}, ΔG_{metal} = -6.03 * S_{metal}, ΔG_{lipo} = -0.117 * S_{lipo} and ΔG_{rot} = 2.56 * H_{rot}

$$\text{ChemScore} = \Delta G_{binding} + DE_{clash} + DE_{int} + DE_{con}$$ **Equation 2**

ChemScores were originated by two types of docking procedures: unconstrained docking and constrained docking. Unconstrained docking served as a preliminary set up, run by keeping all parameters as default,[41] and only changing the radius of the active cavity to 15 Å, in order to accommodate also the largest inhibitors in the dataset. To confirm the ability of the docking function to correctly predict binding poses, the co-crystallized inhibitors (Figure S2) were re-docked into their relative CYP isoform structure. The predicted pose originated from unconstrained docking of three out of four co-crystallized inhibitors was visually comparable with their co-crystallized pose (Figure S3). However, the predicted poses of the selected azole fungicides by unconstrained docking were not comparable to the suggested inhibiting pose of azoles. Specifically, their predicted most energy favorable poses, into the entire active cavity of the selected cytochrome P450 structures, did not consistently position the nitrogen of the azole ring above the heme-iron of the enzyme active site (Figure 1A). Constrained docking was therefore carried out by constraining the distance between the nitrogen in the azole ring and the heme-iron of the enzyme active site. This method positioned the azole molecules into the desired inhibiting pose (Figure 1B), with the distance between the nitrogen and heme-iron approximately within 1 to 2 Å, which is comparable to reported values.[45] This was done by introducing a minimum and maximum separation equal to zero and one, respectively and a spring constant of 10 in the built-in distance constraints options. In both docking procedures, ten poses were generated for each azole structure and the pose with the highest score was considered. An average score was calculated for compounds with two or more stereoisomers.

2.3 Organisms

C. riparius larvae originally obtained from the Swedish University of Agricultural Sciences, Sweden, were cultured based on the OECD Guideline for Testing of Chemicals.[26] During culturing, the organisms were kept in 5 L crystalline dishes containing constantly aerated M7 medium (of approximately 8 cm depth) and quartz sand (of approximately 1 cm depth) at 20 ± 2 °C with 16:8 hour light: dark photoperiods. Evaporated water from the medium was replaced with demineralized water to maintain the ion balance; moreover, 1 L of water was changed once a week to remove excess nutrients. The larvae were fed with 0.15 g of Tubifex® Biotal Basic Vegetable flakes per crystalline dish, three times a week.

L. stagnalis originally obtained from the University of southern Denmark, Denmark, were cultured based on the OECD Guideline for Testing of Chemicals.[25] The organisms used for the following experiments originated from eggs collected from the main culture aquarium two times a week for two weeks and kept in a 12 L aquarium containing constantly aerated tap water and $CaCO_3$ rich sand (of approximately 1 cm depth) at 20 ± 2 °C with 16:8 hour light: dark photoperiods. After hatching, organisms were fed with visually suitable amounts of organic lettuce and Tubifex® Biotal Basic Vegetable flakes, two times a week.

2.4 Chemicals

Azole fungicides used in the present study were bought from Sigma-Aldrich and are summarized in Table 1 together with their type, use, CAS number, purity, molecular weight, predicted logP (computed by Chemicalize,[46] based on Viswanadhan, et al. [47]) and number of isomers. The standard substrate for 7-ethoxycoumarin-O-dealkylase (ECOD) activity of cytochrome P450: 7-ethoxycoumarin (CAS: 31005-02-4, purity: 99.7%) and its product: 7-

hydroxycoumarin (CAS: 93-35-6, purity: 99.5%) were obtained from Sigma-Aldrich. Potassium dihydrogen phosphate (KH_2PO_4, CAS: 7778-770, purity: ≥ 99.0 %) and ethylenediaminetetraacetic acid disodium salt dihydrate (EDTA, CAS: 6381-92-6, purity: 99.0 %) were bought from VWR - Bie & Berntsen. Potassium phosphate dibasic trihydrate ($K_2HPO_4*3H_2O$, CAS: 16788-57-1, purity: ≥ 99.0 %) was obtained from Merck and acetonitrile (ACN, CAS: 75-05-8, purity: ≥ 99.9 %) from Rathburn. Bovine serum albumin (BSA, CAS: 9048-46-8, purity: ≥ 98 %), Bradford reagent (Product nr: M9066), ß-nicotinamide adenine dinucleotide 2'-phosphate reduced tetrasodium salt hydrate (NADPH, CAS: 2646-71-1, purity: ≥ 98 %), 2-methoxyethanol (CAS: 109-86-4, purity: ≥ 99.9 %), DL-dithiothreitol (DTT, CAS: 03-12-3483, purity: ≥ 99.5 %), glycerol (CAS: 56-81-5, purity: ≥ 99 %), phenylmethanesulfonyl fluoride (PMSF, CAS: 329-98-6, purity: ≥ 99.0 %) were obtained from Sigma-Aldrich.

Rat liver microsomes (Product nr: M9066, pooled from male rat) were bought from Sigma-Aldrich. Phosphate buffer (0.30 M) was prepared with KH_2PO_4 (final conc. in buffer: 0.10 M) and $K_2HPO_4*3H_2O$ (final conc. in buffer: 0.20 M) in water from a MilliQ system. Stock solution of 7-ethoxycoumarin (25 mM) was prepared in 30 % v/v ACN in MilliQ water while stock solution of 7-hydroxycoumarin (3.6 mM) in 100 % v/v ACN. The stock solutions of BSA (5 mg mL^{-1}) and NADPH (2 mM) were prepared in phosphate buffer (0.13 M, pH 7.5), of PMSF in 2-methoxyethanol (100 %) and of DTT (50 mM) and EDTA (10 mM) in MilliQ water. Stock solutions of azoles were prepared in 100 % v/v ACN.

2.5 Microsomes preparation

Microsomes were prepared as described in Gottardi, et al. [20]. In short, four instar *C. riparius* larvae (approximately 10 mm in length) or randomly selected *L. stagnalis* (approximately 15 mm in length) were snap frozen in liquid nitrogen and stored at -80 °C. In a single 1.5 mL vial, whole *C. riparius* (5 organisms) larvae or half *L. stagnalis* (after removing the foot, the remaining material was divided into two vials) were homogenized in ice cold homogenization buffer (Tot. vol. 1 mL) containing phosphate buffer (0.13 M, pH 7.5), EDTA (1 mM), PMSF (1 mM), DTT (1 mM) and glycerol (10 % v/v). Homogenization was first performed with a tissue grinder (Econo Grind, Radnoti, U.S.) until the organisms were largely disrupted. After that, further homogenization was carried out with an ultrasonic stick (Digital Sonifier cell disruptor Model 450, Branson Ultrasonics, U.S.) on ice (3 pulses of 3 seconds each, 10 seconds pause between pulses, 20 % amplitude). The homogenate was centrifuged (Optima TM MAX-XP Ultracentrifuge, Beckman Coulter, U.S.) at 10000 g for 15 min at 4 °C; the supernatant was collected and further centrifuged at 100000 g for 50 min at 4 °C. The resulting pellets containing the microsomes were re-suspended (with an ultrasonic stick using 1 to 2 pulses of 3 seconds each, 10 seconds pauses and 10 % amplitude) in 350 µL phosphate buffer (0.13 M, pH 7.5) and glycerol (10 % v/v) on ice. Microsomes obtained from multiple vials were pooled into a single batch and stored at -80 °C.

2.6 Protein content

Protein content was determined according to Bradford [48] by use of a multi-mode microplate reader (SpectraMax i3 Microplate Reader, Molecular Devices, U.S.). Re-suspended microsomes (5 µL) were incubated with 250 µL Bradford reagent at room temperature for 10 – 15 minutes. Absorbance was then measured at 595 nm in a transparent microwell plate (Greiner Bio-one flat

bottom 96-well plate, VWR) and protein content quantified using a bovine serum albumin (BSA) standard dilution series (0 - 1.4 mg protein mL^{-1} BSA in phosphate buffer 0.13 M, pH 7.5).

2.7 Activity and inhibition measurements

Activity measurements were based on the method described by Gottardi, et al. [20] Microsomes from rat-liver (50 µL, final concentration: 0.03 mg microsomal protein mL^{-1}), *C. riparius* (50 µL, final concentration: 0.16 microsomal protein mL^{-1}) and *L. stagnalis* (50 µL, final concentration: 0.16 microsomal protein mL^{-1}) were incubated with phosphate buffer (0.1 M, pH 7.5), NADPH (0.0156 mM for rat liver and 0.025 mM for *C. riparius* and *L. stagnalis*), 7-ethoxycoumarin (0.6 mM for rat liver and 0.3 mM for C. riparius and L. stagnalis) and 5 µL of azole (n = 2 or 3 analytical replicates for rat liver, n = 3 for *C. riparius* and *L. stagnalis*) or 5 µL solvent (control, n = 2 or 3 analytical replicates for rat liver, n = 6 for *C. riparius* and n = 4 for *L. stagnalis*) in a total volume of 255 µL. Blanks were made with all reagents except the substrate in order to account for background fluorescence of NADPH[49] and with re-suspended microsomes (50 µL) in order to maintain the same density and fluorescence attenuation of the medium. Fluorescence increase due to 7-hydroxycoumarin formation (excitation: 380 nm, emission: 480 nm) was measured every 30 seconds for 30 minutes for rat liver or every 1 minute for 60 minutes for *C. riparius* and *L. stagnalis* in a black microwell plate (BRANDplates® pureGrade™, Brand, Germany) with a multi-mode microplate reader (SpectraMax i3 Microplate Reader, Molecular Devices, U.S.) at 37 °C.

Measurements of inhibition with rat liver microsomes were carried out with all the 18 azoles selected in the present study, out of those, the 5 imidazoles and the 6 and 5 most potent triazoles

were selected for measurements of inhibition in *C. riparius* and *L. stagnalis* microsomes, respectively.

2.8 Experimental determination of inhibition strength (half maximal inhibitory concentrations, IC_{50})

Fluorescence measured over time was corrected by subtracting the average fluorescence measured in the blanks over time. Cytochrome P450 activity (change in fluorescence per unit of time) was determined as the slope of a linear regression fitted with Sigma Plot version 13 (Systat) in the linear range of fluorescent product formation.

7-ethoxycoumarin-O-dealkylase (ECOD) activity in the presence of an inhibitor was expressed as percentages relative to control activity (without the addition of azole fungicide, 100 % activity). Estimation of half maximal inhibitory concentration (IC_{50}) was carried out by fitting a two parameters log-logistic model (Equation 3) in RStudio version 1.0.143 with the drc-package.[50]

$$y = \frac{100}{1+\left(\frac{x}{IC_{50}}\right)^{b}}$$ **Equation 3**

where x is the concentration of inhibitor (μM), y is the ECOD activity relative to control (in percent), IC_{50} is the half maximal inhibitory concentration (in μM) and b is a factor describing the slope around IC_{50}.

Background control activities were quantified with measurements of product (7-hydroxycoumarin) fluorescence and converted to pmol min^{-1} mg microsomal $protein^{-1}$ by

conversion factors of 1.79 10^5, 1.59 10^5 and 1.86 10^5 relative fluorescence units $pmol^{-1}$, for rat, *C. riparius* and *L. stagnalis*, respectively.

2.9 Statistical analysis

The estimated IC_{50} values were log-transformed prior to any analysis in order to obtain normal distribution around the mean. Normal distribution around the mean of estimated IC_{50} values and docking scores were checked with the Kolmogorov-Smirnov test (normal distribution with $p>0.05$). Correlations between estimated IC_{50} values and docking scores were analysed with Pearson (parametric test) or Spearman (non-parametric) test in case of normally or not normally distributed docking scores, respectively (significant correlations with $p<0.05$). Differences between correlations were analysed with Fisher Z-test for equality of correlations (significant differences with $p<0.05$). Regression analysis between the estimated IC_{50} values in rat liver, *C. riparius* and *L. stagnalis* was carried out after checking for equality of variances (F test, equal variances with $p>0.05$). Mystat version 12.02.00 (Systat) was used for all statistical analysis.

3 Results and discussion

3.1 *In silico* estimated affinities and correlation to rat liver cytochrome P450 inhibition

Unconstrained docking predicted the most energy favorable pose of the azole fungicides into the entire active cavity of the selected cytochrome P450 structures while constrained docking positioned the azoles into their inhibiting pose, allowing the estimation of affinities between the azoles in their inhibiting pose and the space adjacent to the reaction site. Unconstrained docking scores are on average 19 ChemScore units higher than constrained docking scores, generally due to higher predicted penalties for constrained docking as compared to unconstrained docking (data

not shown). Docking scores originating from unconstrained and constrained docking are strongly correlated to each other for all cytochrome P450 structures used ($0.709 < r < 0.987$, $p < 0.05$; Figure S3). Nonetheless, due to the particular biological relevance of the constrained poses, as compared to the apparently irrelevant unconstrained poses when investigating inhibition strengths of azole fungicides, only constrained docking scores are considered in the following.

Docking scores of selected azoles vary for up to 25 ChemScore units from each other within a single cytochrome P450 structure (Table S4). Moreover, docking scores of a single azole vary for up to 46 ChemScore units between different cytochrome P450 structures (Table S4). This suggests the ability of the present model to identify differences among the selected azoles as well as between the cytochrome P450 structures used. Nonetheless, docking scores are strongly correlated to one another across all cytochrome P450 structures used ($0.527 < r < 0.980$, $p < 0.05$; Figure S4 and S5) and anticorrelate strongly and significantly with the experimentally determined inhibition strengths (IC_{50}) in rat liver ($-0.662 < r < -0.891$, $p < 0.05$; Figure 2), with exception of clotrimazole. The correlations between docking scores and measured inhibition strengths are not significantly different among one another (Z-test, $p>0.05$), among the different cytochrome P450 isoforms or structures used. Furthermore, the correlations are only marginally stronger (on average 3 to 9 % higher correlation coefficients) for the enzymatic structures crystallized with an inhibitor (CYP2C9 4NZ2, CYP3A4 2V0M and CYP2D6 4XRZ), as compared to their counterpart with no co-crystallized inhibitor (CYP2C9 1R9O, CYP3A4 1TQN and CYP2D6 2F9Q). Taken together, the choice of neither a specific cytochrome P450 isoform nor a specific crystallized structure within the same isoform has a significant effect on the correlations obtained between docking scores and measured inhibition strengths, supporting the

hypothesis that the affinities between the selected azoles and cytochrome P450 isoforms are strongly correlated to one another.

Although not significantly different among one another, the correlation between docking scores and measured inhibition strengths are strongest for the human CYP2C9 (r: -0.891 for structure 4NZ2 and r: -0.835 for structure 1R9O), followed by human CYP3A4 (r: -0.859 for structure 2V0M and r: -0.835 for structure 1TQN) and fungal CYP51 (r: -0.824) and weakest for human CYP2D6 (r: -0.721 for structure 4XRZ and r: -0.662 for structure 2F9Q). This seems to agree with the relative size of human cytochrome P450 active cavities, being largest for CYP2C9 and CYP3A4 and relatively smaller for CYP2D6, and with the lipophilicity of the active pockets, being highest for CYP2C9, followed by CYP3A4 and lastly 2D6.[22]

In order to examine which interactions are predicted to play the major contribution to the docking scores of the selected azoles toward the cytochrome P450 structures, the correlations between scores and scoring function single terms (Equation 1 and Equation 2) were analysed (Tables S5 – S11 and Figures S6 – S12). The predicted metal interaction (S_{metal}, Equation 1) is equal for all azole fungicides structures and it has a value of 0 or 0.9 depending on the cytochrome P450 structure used for docking. This is possibly due to lack of resolution of the scoring function. Conversely, the predicted lipophilic interaction (S_{lipo}, Equation 1) is the term which correlates the most with the docking scores for all cytochrome P450 structures used ($0.433 < r < 0.966$, $p < 0.05$). The term is based on the number of non-polar carbon, non-accepting sulphur, non-ionic bromine, chlorine and iodine atoms of the ligand and the enzymatic active site,[42, 43] therefore depending strongly on the nature of their three-dimensional structures. This is in agreement with the reported strong correlation between azole affinities toward CYP3A and CYP2B and their lipophilicity expressed as logP (pIC_{50} and logP, r: 0.988).[51] In the present study

and in the context of the scoring function used, we conclude that *in silico* estimated affinities of the selected azoles depends mainly on their ability to lipophilically interact with the enzyme active cavities.

3.2 *In silico* estimated affinities and extrapolation to insects and molluscs

Correlations between docking scores and experimentally determined inhibition strengths (IC_{50}) in *C. riparius* are weaker than those for rat liver ($-0.286 < r < -0.733$; Figure 3) and significant for one of the seven cytochrome P450 structure tested ($p > 0.05$ except for CYP2C9 4NZ2). This may be due to a hypothetical more similar composition and/or susceptibility of cytochrome P450s between humans and rats, as compared to humans and insects.[15, 52, 53] Moreover, the correlations is even weaker and not significant for *L. stagnalis* ($-0.084 < r < -0.593$, $p > 0.05$; Figure 4). In addition to clotrimazole, ketoconazole presents outlier behaviour in both species. *In silico* estimated affinities seem able to correctly rank azole fungicides in terms of their inhibition strength toward cytochrome P450 activities of rat liver, and to a lesser extent of *C. riparius*, while failing in the case of *L. stagnalis*. This rejects the hypothesis that *in silico* estimated affinities can be used to rank azole fungicides inhibition strengths toward cytochrome P450 activities equally well in different species.

3.3 Comparing measured inhibition strengths between species

In the present study, measured background ECOD activity of rat liver is equal to 625 pmol min^{-1} mg microsomal $protein^{-1}$, background *C. riparius* activity ranges between 5 and 29 pmol min^{-1} mg microsomal $protein^{-1}$ in different microsomes batches, while background activity of *L. stagnalis* is 8 pmol min^{-1} mg microsomal $protein^{-1}$. This suggests comparable degrees of activities between *C. riparius* and *L. stagnalis* and 20 to 125-folds higher activities in rat liver

microsomes as compared to the other two species. Comparable cytochrome P450 ECOD activities have been reported for rat liver microsomes (approximately 2000 pmol min^{-1} mg microsomal $protein^{-1}$),[54] as well as *C. riparius* (0.5 to 1 pmol min^{-1} mg microsomal $protein^{-1}$),[55] while reported cytochrome P450 ECOD activities seem to be lacking for *L. stagnalis*. The reason for the difference in enzymatic activity per microsomal protein of rat as compared to invertebrates is most likely that rat microsomes are isolated from the liver, known to be the organ with one of the highest concentrations of detoxification enzymes, while invertebrate microsomes are isolated from whole organisms.

The ability of the selected azole fungicides to inhibit measured cytochrome P450 activity depends both on the azole fungicide and the selected species (Table 1 and dose response curves in Figures S10, S11 and S12). Comparable inhibitory concentrations in the μM range have been previously reported towards rat liver CYP2B and CYP3A activities,[51] fungal growth [37] and human as well as fish aromatase (CYP19).[1] On the other hand, inhibition of microsomal cytochrome P450 activity of *C. riparius* and *L. stagnalis* due to azole fungicides is, to the best of our knowledge, not yet available. IC_{50} values for rat liver (0.0032 – 26 μM) and *C. riparius* (0.074 – 18 μM) are within the same range. *L. stagnalis* microsomes presents up to three orders of magnitude higher IC_{50} values (2.3 – 142 μM) as compared to rat liver and *C. riparius* (Table 1), showing lower susceptibility toward inhibition by azoles as compared to the two other species.

Inhibition strengths of the selected azole fungicides measured in *C. riparius* are strongly correlated to the strengths measured in rat liver (r: 0.857, p: 0.002; Figure 5). It seems possible to extrapolate the relative strengths of azole fungicides toward cytochrome P450 activity in *C. riparius* from measurements carried out in rat liver, as approximately 70% of the variation in *C.*

riparius can be described by the measurements in rat liver (R^2: 0.734, Figure 5). On the other hand, as expected, no significant relationship is found between inhibition strengths toward rat liver and *L. stagnalis* or toward *C. riparius* and *L. stagnalis* (Figure 5), rejecting the hypothesis that the measured inhibition strengths of azole fungicides toward microsomal cytochrome P450 activities can be extrapolated between species of different phyla.

3.4 Method limitations

The variation between the estimated *in silico* affinities and measured inhibition strengths of the selected azoles against cytochrome P450 activity of different organisms can have several causes, due to a number of aspects not accounted for by the models used in the present study.

The substrate 7-ethoxycoumarin, shown to be unspecific for human cytochrome P450s involved in detoxification,[56] should cover the activity of several cytochrome P450 isoforms. However, to the best of our knowledge, its selectivity for cytochrome P450 isoforms present in *C. riparius* and *L. stagnalis* is unknown. The specific cytochrome P450(s) able to metabolize the substrate 7-ethoxycoumarin in the different species may present substantial differences. Therefore, azoles may inhibit cytochrome P450 catalyzed oxidations not measured with the selected *in vitro* model, as for example hydroxylation reactions or may inhibit diverse cytochrome P450s with ECOD activities in the different species, adding uncertainties to the measured inhibition strengths and their inter-species correlations.

The majority of the azole fungicides selected has several stereoisomers. It has been reported that the binding affinities and inhibition strengths among stereoisomers may be different, depending on their structural differences and/or the target enzymatic system/organism.[37, 57, 58] In the present study, docking scores of stereoisomers varies for up to 11 ChemScore units from

each other (Table S2 and S4). However, measurements of inhibition strengths are carried out with racemic mixtures, so it is not possible to compare estimated affinity and inhibition strength of each separate stereoisomer. It is important to keep in mind that the relative part played by each stereoisomer toward inhibition may be different, adding uncertainties to the correlation between measured inhibition strengths and estimated affinities of racemic mixtures.

Metabolism of azole fungicides may have taken place already during measurements of inhibition strengths in rat liver microsomes as well as in the microsomes extracted from *C. riparius* and *L. stagnalis*, as azole fungicides have been reported to be readily metabolized by rat liver microsomes.[59] The potential formation of metabolites which are able to interact with cytochrome P450s more or less potently than the parent compound adds further uncertainties to measurement of inhibition strengths and estimated affinities. This may explain the different inhibition strengths of clotrimazole and ketoconazole toward cytochrome P450 activity among the different species, and their resulting outlier behaviour (Figure 2, 3, 4 and 5). In particular, docking scores of clotrimazole toward the selected cytochrome P450 structures are generally underestimated as compared to the inhibition strength and are much lower than the scores of the other imidazoles (approximately 60 to 250 % lower than the average of all imidazoles for five out of the seven cytochrome P450 structures used). The low docking scores seems to be due to high clashing terms (DE_{clash}, Equation 2) and/or absence or low hydrogen bond interaction ($S_{hbond,}$ Equation 2; Table S6, S7, S8, S9 and S10). The discrepancy observed between docking scores and inhibition strength of clotrimazole may be due to formation of metabolites with higher affinity and consequential stronger inhibition strength toward cytochrome P450 activity than estimated for the parent compound. In the present study, however, even though cytochrome P450 structures are selected with or without the presence of a co-crystallized inhibitor, the *in silico*

model does not directly consider the flexibility of cytochrome P450 active cavities. It has been previously reported for mammalian cytochrome P450s,[60] that the position of structural elements in the active cavity can change upon ligand binding. In the real situation, this may reduce any predicted clash due to close molecular contacts and allow even the relatively larger and more cumbersome ligands to be accommodated into the active pocket.

Docking scores of ketoconazole are overestimated as compared to its inhibition strength in *C. riparius* and *L. stagnalis* (Figure 3 and 4) but not in rat liver (Figure 2). The compound is the largest molecule investigated and has the highest docking scores among all azoles in the present study (Table S2 and S4) independently on which cytochrome P450 structure is used for docking. Its inhibition strength is different among the species, approximately 50 % to four orders of magnitude weaker toward activities in *C. riparius* and *L. stagnalis* than toward rat liver. The observed behaviour may be due to differences in the susceptibility of cytochrome P450s of rat and the two invertebrate species toward ketoconazole inhibition. However, this cannot be estimated by the present model, as *in silico* affinities are estimated with human and fungal cytochrome P450 structures.

Experimental determination of very high inhibition strengths, such as those found for clotrimazole and ketoconazole, may be subject to large uncertainties due to experimental procedures and biological variation. In order to test experimental variability of the measured inhibition strengths, measurements of IC_{50} with imidazoles were repeated in rat liver microsomes with a different batch and chemical stock solutions. The new values are comparable to the previous, being in the same order of magnitude and presenting the same ranking among the five imidazoles tested (bifonazole: 0.19±0.03 μM, clotrimazole: 0.004±0.003 μM, imazalil: 0.54± μM, ketoconazole: 0.28±0.09 μM and prochloraz: 0.37±0.07 μM) (Figure S16) thus showing an

acceptable inter-experimental variability when measuring low inhibition strengths with the current method.

Conclusions

Taken together, the use of *in vitro* measurements with commercially available rat liver microsomes and to a lesser extent *in silico* estimated affinities seems to be a promising tool to identify inhibition of cytochrome P450 activity by azoles in *C. riparius*. On the other hand, *L. stagnalis* presents a very different enzymatic susceptibility toward azole inhibition and no extrapolation from either measurement in rat liver or estimated *in silico* affinities can be made. At present, only direct measurements of cytochrome P450 activity *in vitro* for *L. stagnalis* can be used to estimate inhibition strengths of azole fungicides in this species. Moreover, it is still an open question whether the suggested applicability of *in silico* and *in vitro* models for *C. riparius* holds for other species, or if the observed unsuitability for *L. stagnalis* is the norm, rather than the exception.

Author Contributions

The manuscript was written through contributions of all authors. All authors have given approval to the final version of the manuscript.

Funding Sources

University of Copenhagen, Copenhagen, Denmark. The funding source had no involvement in study design; in the collection, analysis and interpretation of data; in the writing of the report; nor in the decision to submit the article for publication.

Declarations of interest: none

ACKNOWLEDGMENT

The authors thank Eirini Apazoglou for her work on rat liver microsomes, Michala Rosa Birch for culturing and pilot measurements in *L. stagnalis*, Giulia Bellisai and Anja Weibell for culturing *C. riparius*. The authors are also grateful to Azedine Zoufir and Fredrik Svensson for their support on the *in silico* model.

REFERENCES

1. Saxena, A. K.; Devillers, J.; Bhunia, S. S.; Bro, E., Modelling inhibition of avian aromatase by azole pesticides. *Sar and Qsar in Environmental Research* **2015,** *26*, (7-9), 757-782.

2. Kahle, M.; Buerge, I. J.; Hauser, A.; Müller, M. D.; Poiger, T., Azole fungicides: Occurrence and fate in wastewater and surface waters. *Environmental Science & Technology* **2008,** *42*, (19), 7193-7200.

3. Riise, G.; Lundekvam, H.; Wu, Q. L.; Haugen, L. E.; Mulder, J., Loss of pesticides from agricultural fields in SE Norway - runoff through surface and drainage water. *Environmental Geochemistry and Health* **2004,** *26*, (2-3), 269-276.

4. Werner, I.; Zalom, F. G.; Oliver, M. N.; Deanovic, L. A.; Kimball, T. S.; Henderson, J. D.; Wilson, B. W.; Krueger, W.; Wallender, W. W., Toxicity of storm-water runoff after dormant spray application in a French prune orchard, Glenn County, California, USA: Temporal patterns and the effect of ground covers. *Environmental Toxicology and Chemistry* **2004,** *23*, (11), 2719-2726.

5. Bjergager, M. B. A.; Dalhoff, K.; Kretschmann, A.; Norgaard, K. B.; Mayer, P.; Cedergreen, N., Determining lower threshold concentrations for synergistic effects. *Aquatic Toxicology* **2017,** *182*, 79-90.

6. Copping, L. G.; Hewitt, H. G., Fungicides. In *Chemistry and Mode of Action of Crop Protection Agents*, Copping, L. G.; Hewitt, H. G., Eds. The Royal Society of Chemistry: 1998; pp 74-113.

7. Maertens, J. A., History of the development of azole derivatives. *Clinical Microbiology and Infection* **2004,** *10*, 1-10.

8. Pilling, E. D.; Bromleychallenor, K. A. C.; Walker, C. H.; Jepson, P. C., Mechanism of synergism between the pyrethroid insecticide lambda-cyhalothrin and the imidazole fungicide prochloraz, in the honeybee (*Apis-mellifera* L.). *Pesticide Biochemistry and Physiology* **1995,** *51*, (1), 1-11.

9. Bach, J.; Snegaroff, J., Effects of the fungicide prochloraz on xenobiotic metabolism in Rainbow trout - *in vivo* induction. *Xenobiotica* **1989,** *19*, (1), 1-9.

10. Snegaroff, J.; Bach, J., Effects of the fungicide prochloraz on xenobiotic metabolism in rainbow trout: inhibition *in vitro* and time course of induction *in vivo*. *Xenobiotica* **1989,** *19*, (3), 255-67.

11. Cedergreen, N., Quantifying synergy: A systematic review of mixture toxicity studies within environmental toxicology. *PLoS ONE* **2014,** *9*, (5), e96580.

12. Belden, J. B.; Lydy, M. J., Impact of atrazine on organophosphate insecticide toxicity. *Environmental Toxicology and Chemistry* **2000,** *19*, (9), 2266-2274.

13. Correia, M.; Ortiz de Montellano, P., Inhibition of cytochrome P450 enzymes. In *Cytochrome P450*, Ortiz de Montellano, P., Ed. Springer US: 2005; pp 247-322.

14. James, M. O.; Boyle, S. M., Cytochromes P450 in crustacea. *Comparative Biochemistry and Physiology C-Pharmacology Toxicology & Endocrinology* **1998,** *121*, (1-3), 157-172.

15. Rewitz, K. F.; Styrishave, B.; Lobner-Olesen, A.; Andersen, O., Marine invertebrate cytochrome P450: Emerging insights from vertebrate and insect analogies. *Comparative Biochemistry and Physiology C-Toxicology & Pharmacology* **2006,** *143*, (4), 363-381.

16. Snyder, M. J., Aquatic P450 Species. In *The Ubiquitous Roles of Cytochrome P450 Proteins*, Sigel, A.; Sigel, H.; Sigel, R. K. O., Eds. John Wiley & Sons, Ltd: 2007; pp 97-126.

17. Koymans, L.; Kelder, G. M. D. D.; Te, J. M. K.; Vermeulen, N. P. E., Cytochromes P450: Their active-site structure and mechanism of oxidation. *Drug Metabolism Reviews* **1993,** *25*, (3), 325-387.

18. Poulos, T.; Johnson, E., Structures of cytochrome P450 enzymes. In *Cytochrome P450*, Ortiz de Montellano, P., Ed. Springer US: 2005; pp 87-114.

19. Aitio, A., A simple and sensitive assay of 7-ethoxycoumarin deethylation. *Analytical Biochemistry* **1978,** *85*, (2), 488-491.

20. Gottardi, M.; Kretschmann, A.; Cedergreen, N., Measuring cytochrome P450 activity in aquatic invertebrates: a critical evaluation of *in vitro* and *in vivo* methods. *Ecotoxicology* **2015,** *25*, (2), 419-430.

21. de Graaf, C.; Vermeulen, N. P. E.; Feenstra, K. A., Cytochrome P450 *in silico*: An integrative modeling approach. *Journal of Medicinal Chemistry* **2005,** *48*, (8), 2725-2755.

22. Kirchmair, J.; Williamson, M. J.; Tyzack, J. D.; Tan, L.; Bond, P. J.; Bender, A.; Glen, R. C., Computational prediction of metabolism: sites, products, SAR, P450 enzyme dynamics, and mechanisms. *Journal of Chemical Information and Modeling* **2012,** *52*, (3), 617-48.

23. Gilbert D; Singan VR; Colbourne JK, wFleaBase: the Daphnia genomics information system. In BMC Bioinformatics 2005, 6:45 doi: 10.1186/1471-2105/6/45: Available online via: http://wfleabase.org/

24. Meunier, B.; de Visser, S. P.; Shaik, S., Mechanism of oxidation reactions catalyzed by cytochrome P450 enzymes. *Chemical Reviews* **2004,** *104*, (9), 3947-3980.

25. OECD, Test no. 243: *Lymnaea stagnalis* reproduction test. In *OECD Guidelines for the testing of chemicals, section 2: Effects on biotic systems*, Organisation for Economic Co-operation and Development: 2016.

26. OECD, Test no. 235: *Chironomus* sp., acute immobilisation test. In *OECD Guidelines for the testing of chemicals, section 2: Effects on biotic systems*, Organisation for Economic Co-operation and Development: 2011.

27. Kim, S.; Thiessen, P. A.; Bolton, E. E.; Chen, J.; Fu, G.; Gindulyte, A.; Han, L.; He, J.; He, S.; Shoemaker, B. A.; Wang, J.; Yu, B.; Zhang, J.; Bryant, S. H., PubChem substance and compound databases. *Nucleic Acids Research* **2016,** *44*, (D1), D1202-13.

28. Irwin, J. J.; Sterling, T.; Mysinger, M. M.; Bolstad, E. S.; Coleman, R. G., ZINC: A free tool to discover chemistry for biology. *Journal of Chemical Information and Modeling* **2012,** *52*, (7), 1757-1768.

29. Berman, H. M.; Westbrook, J.; Feng, Z.; Gilliland, G.; Bhat, T. N.; Weissig, H.; Shindyalov, I. N.; Bourne, P. E., The Protein Data Bank. *Nucleic Acids Research* **2000,** *28*, (1), 235-242.

30. Roy, K.; Roy, P. P., QSAR of cytochrome inhibitors. *Expert Opinion on Drug Metabolism & Toxicology* **2009,** *5*, (10), 1245-1266.

31. Yano, J. K.; Wester, M. R.; Schoch, G. A.; Griffin, K. J.; Stout, C. D.; Johnson, E. F., The structure of human microsomal cytochrome P450 3A4 determined by X-ray crystallography to 2.05-A resolution. *The Journal of Biological Chemistry* **2004,** *279*, (37), 38091-4.

32. Tyzack, J. D.; Williamson, M. J.; Torella, R.; Glen, R. C., Prediction of cytochrome P450 xenobiotic metabolism: Tethered docking and reactivity derived from ligand molecular orbital analysis. *Journal of Chemical Information and Modeling* **2013,** *53*, (6), 1294-1305.

33. Ekroos, M.; Sjogren, T., Structural basis for ligand promiscuity in cytochrome P450 3A4. *Proceedings of the National Academy of Sciences of the United States of America* **2006,** *103*, (37), 13682-7.

34. Wester, M. R.; Yano, J. K.; Schoch, G. A.; Yang, C.; Griffin, K. J.; Stout, C. D.; Johnson, E. F., The structure of human cytochrome P450 2C9 complexed with flurbiprofen at 2.0-A resolution. *The Journal of Biological Chemistry* **2004,** *279*, (34), 35630-7.

35. Branden, G.; Sjogren, T.; Schnecke, V.; Xue, Y., Structure-based ligand design to overcome CYP inhibition in drug discovery projects. *Drug Discovery Today* **2014,** *19*, (7), 905-11.

36. Brodney, M. A.; Beck, E. M.; Butler, C. R.; Barreiro, G.; Johnson, E. F.; Riddell, D.; Parris, K.; Nolan, C. E.; Fan, Y.; Atchison, K.; Gonzales, C.; Robshaw, A. E.; Doran, S. D.; Bundesmann, M. W.; Buzon, L.; Dutra, J.; Henegar, K.; LaChapelle, E.; Hou, X. J.; Rogers, B. N.; Pandit, J.; Lira, R.; Martinez-Alsina, L.; Mikochik, P.; Murray, J. C.; Ogilvie, K.; Price, L.; Sakya, S. M.; Yu, A. J.; Zhang, Y.; O'Neill, B. T., Utilizing structures of CYP2D6 and BACE1 complexes to reduce risk of drug-drug interactions with a novel series of centrally efficacious BACE1 inhibitors. *Journal of Medicinal Chemistry* **2015,** *58*, (7), 3223-3252.

37. Tyndall, J. D. A.; Sabherwal, M.; Sagatova, A. A.; Keniya, M. V.; Negroni, J.; Wilson, R. K.; Woods, M. A.; Tietjen, K.; Monk, B. C., Structural and functional elucidation of yeast lanosterol 14 alpha-demethylase in complex with agrochemical antifungals. *Plos One* **2016,** *11*, (12).

38. *Maestro. version 2014-2*, Schrodinger, LLC, New York, NY, 2014.

39. Jones, G.; Willett, P.; Glen, R. C.; Leach, A. R.; Taylor, R., Development and validation of a genetic algorithm for flexible docking. *Journal of Molecular Biology* **1997,** *267*, (3), 727-748.

40. *GOLD. version 5.4*, Cambridge Crystallographic Data Center, CCDC Software Ltd., Cambridge, UK, 2015.

41. *GOLD User Guide, A component of the GOLD suite*, Cambridge Crystallographic Data Centre, CCDC Software Ltd., available at https://www.ccdc.cam.ac.uk/support-and-resources/ccdcresources/gold.pdf, 2015.

42. Baxter, C. A.; Murray, C. W.; Clark, D. E.; Westhead, D. R.; Eldridge, M. D., Flexible docking using Tabu search and an empirical estimate of binding affinity. *Proteins-Structure Function and Genetics* **1998,** *33*, (3), 367-382.

43. Eldridge, M. D.; Murray, C. W.; Auton, T. R.; Paolini, G. V.; Mee, R. P., Empirical scoring functions .1. The development of a fast empirical scoring function to estimate the binding affinity of ligands in receptor complexes. *Journal of Computer-aided Molecular Design* **1997,** *11*, (5), 425-445.

44. Kirton, S. B.; Murray, C. W.; Verdonk, M. L.; Taylor, R. D., Prediction of binding modes for ligands in the cytochromes P450 and other heme-containing proteins. *Proteins-Structure Function and Bioinformatics* **2005,** *58*, (4), 836-844.

45. Balding, P. R.; Porro, C. S.; McLean, K. J.; Sutcliffe, M. J.; Marechal, J. D.; Munro, A. W.; de Visser, S. P., How do azoles inhibit cytochrome P450 enzymes? A density functional study. *Journal of Physical Chemistry A* **2008,** *112*, (50), 12911-12918.

46. *Chemicalize*, developed by ChemAxon, available at http://www.chemaxon.com, 2016.

47. Viswanadhan, V. N.; Ghose, A. K.; Revankar, G. R.; Robins, R. K., Atomic physicochemical parameters for 3 dimensional structure directed quantitative structure - activity relationships. 4. Additional parameters for hydrophobic and dispersive interactions and their application for an automated superposition of certain naturally-occurring nucleoside antibiotics. *Journal of Chemical Information and Computer Sciences* **1989,** *29*, (3), 163-172.

48. Bradford, M. M., A rapid and sensitive method for the quantitation of microgram quantities of protein utilizing the principle of protein-dye binding. *Analytical Biochemistry* **1976,** *72*, (1–2), 248-254.

49. Aitio, A., A simple and sensitive assay of 7-ethoxycoumarin deethylation. In *Toxicological Aspects of Food Safety*, Leonard, B. J., Ed. Springer Berlin Heidelberg: 1978; Vol. 1, pp 275-275.

50. Ritz, C.; Streibig, J. C., Bioassay analysis using R. *Journal of Statistical Software* **2005,** *12*, (5), 1-22.

51. Itokawa, D.; Nishioka, T.; Fukushima, J.; Yasuda, T.; Yamauchi, A.; Chuman, H., Quantitative structure-activity relationship study of binding affinity of azole compounds with CYP2B and CYP3A. *Qsar & Combinatorial Science* **2007,** *26*, (7), 828-836.

52. Snyder, M. J., Cytochrome P450 enzymes in aquatic invertebrates: recent advances and future directions. *Aquatic Toxicology* **2000,** *48*, (4), 529-547.

53. Baldwin, W. S.; Marko, P. B.; Nelson, D. R., The cytochrome P450 (CYP) gene superfamily in *Daphnia pulex*. *Bmc Genomics* **2009,** *10*.

54. Moon, J. Y.; Lee, D. W.; Park, K. H., Inhibition of 7-ethoxycoumarin O-deethylase activity in rat liver microsomes by naturally occurring flavonoids: structure-activity relationships. *Xenobiotica* **1998,** *28*, (2), 117-126.

55. Sturm, A.; Hansen, P. D., Altered cholinesterase and monooxygenase levels in *Daphnia magna* and *Chironomus riparius* exposed to environmental pollutants. *Ecotoxicology and Environmental Safety* **1999,** *42*, (1), 9-15.

56. Waxman, D. J.; Chang, T. K., Use of 7-ethoxycoumarin to monitor multiple enzymes in the human CYP1, CYP2, and CYP3 families. *Methods in Molecular Biology* **2006,** *320*, 153-6.

57. Lamb, D. C.; Kelly, D. E.; Baldwin, B. C.; Gozzo, F.; Boscott, P.; Richards, W. G.; Kelly, S. L., Differential inhibition of *Candida albicans* CYP51 with azole antifungal stereoisomers. *FEMS Microbiology Letters* **1997,** *149*, (1), 25-30.

58. Stehmann, C.; De Waard, M. A., Relationship between chemical structure and biological activity of triazole fungicides against *Botrytis cinerea*. *Pesticide Science* **1995,** *44*, (2), 183-195.

59. Fabian, E.; Wang, X.; Engel, F.; Li, H.; Landsiedel, R.; van Ravenzwaay, B., Activities of xenobiotic metabolizing enzymes in rat placenta and liver in vitro. *Toxicology In Vitro : An International Journal Published in Association with Bibra* **2016,** *33*, 174-9.

60. Yu, X. F.; Cojocaru, V.; Wade, R. C., Conformational diversity and ligand tunnels of mammalian cytochrome P450s. *Biotechnology and Applied Biochemistry* **2013,** *60*, (1), 134-145.

FIGURES

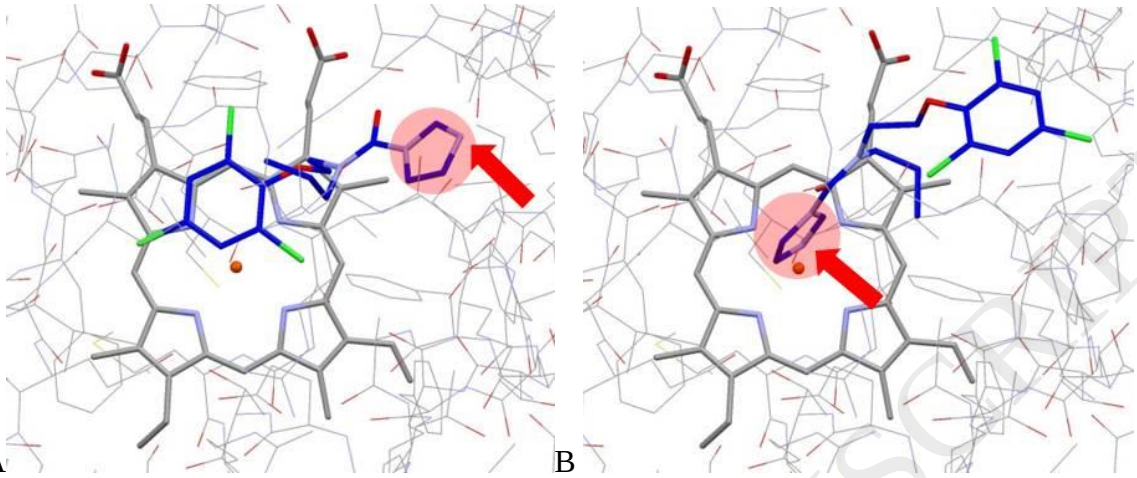

A B

[COLORED FIGURE]

Figure 1. Examples of the predicted pose of an azole fungicide (prochloraz) docked into a cytochrome P450 active pocket (CYP3A4 PDB 2V0M) with unconstrained (A) and constrained docking (B). Note that with constrained docking, the nitrogen (indicated by the red arrow) of the azole ring (red shaded circle) is positioned directly above the heme-iron (orange sphere), resembling the suggested inhibiting pose of azole fungicides. Oxygen, chlorine and nitrogen atoms are represented by red, green and light-blue thick sticks. The carbon atoms in the cytochrome P450 structure and heme-group are represented by thin or thick gray sticks, respectively. The carbon atoms in the azole molecule are represented by thick dark-blue sticks.

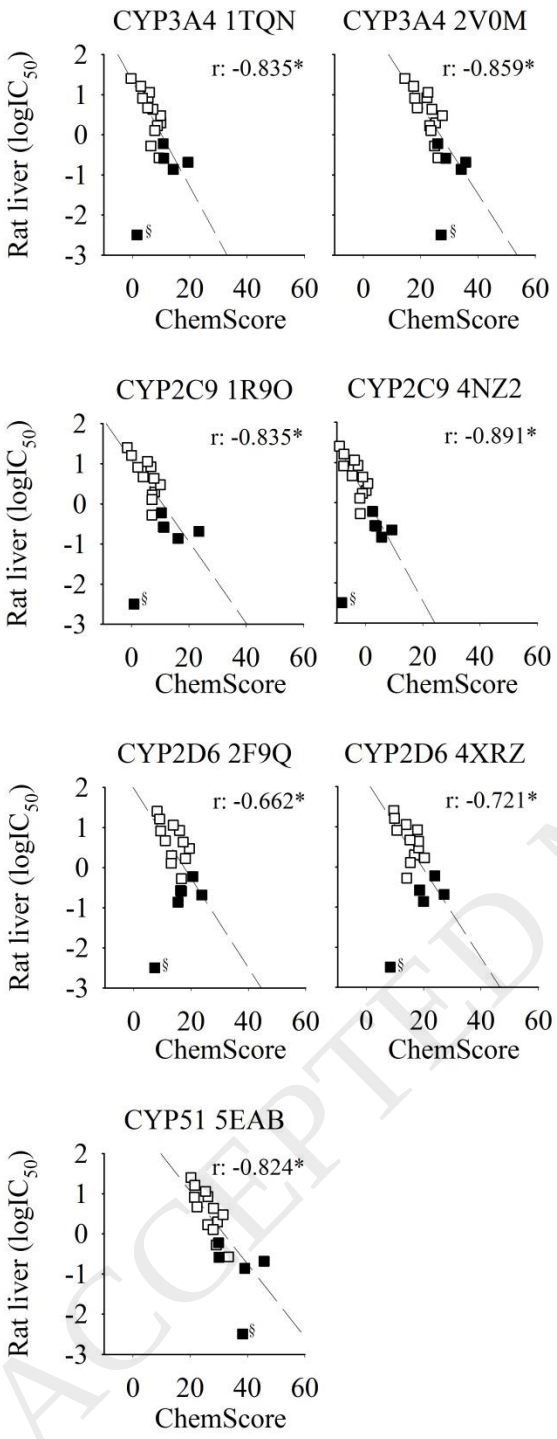

Figure 2. Correlations between inhibition strengths of triazole fungicides (white symbols) and imidazole fungicides (black symbols) toward rat liver ECOD activity (in $logIC_{50}$ μM) (n = 17) and docking scores obtained with constrained docking into human CYP2C9, CYP2D6 and

CYP3A4 and fungal CYP51. “r” denotes Pearson correlation coefficients. * denotes a statistically significant correlation. Correlations were not found to be significantly different among one another (Z test, $p > 0.05$). Clotrimazole (§) was not included in the correlation analysis.

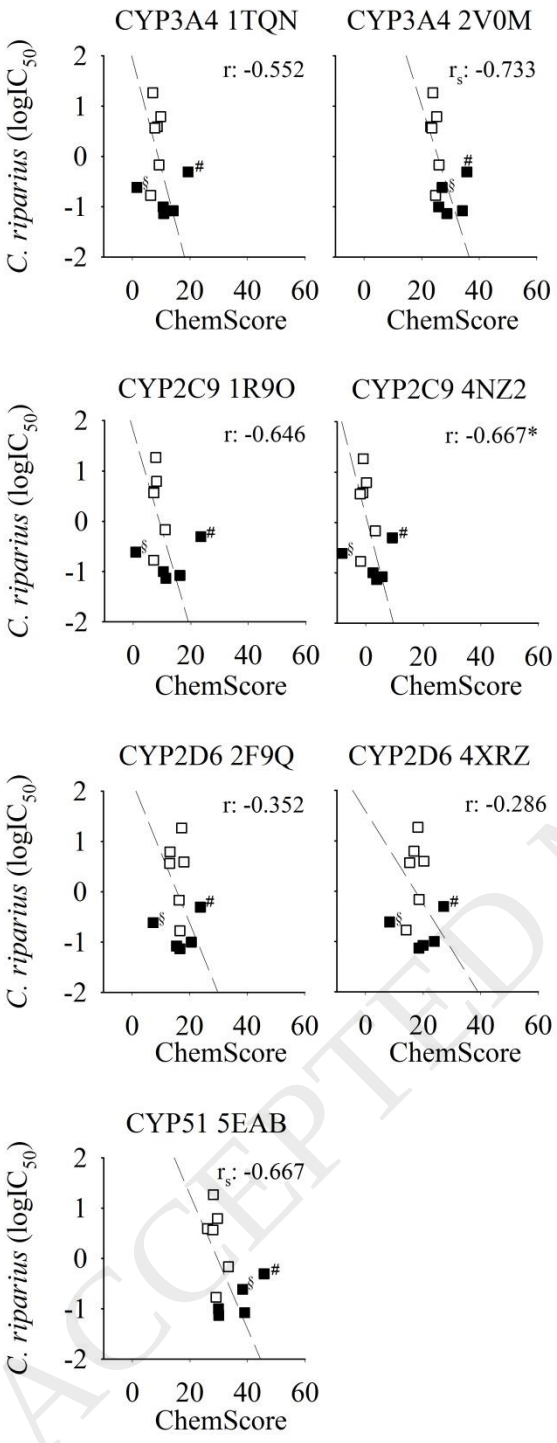

Figure 3. Correlations between inhibition strengths of triazole fungicides (white symbols) and imidazole fungicides (black symbols) toward *C. riparius* (n = 9) ECOD activity (in $logIC_{50}$ μM) and docking scores obtained with constrained docking into human CYP2C9, CYP2D6 and

CYP3A4 and fungal CYP51. "r" and "r_{sp}" denote Pearson or Spearman correlation coefficients, respectively. * denotes a statistically significant correlation. Clotrimazole (§) and ketoconazole (#) were not included in the correlation analysis.

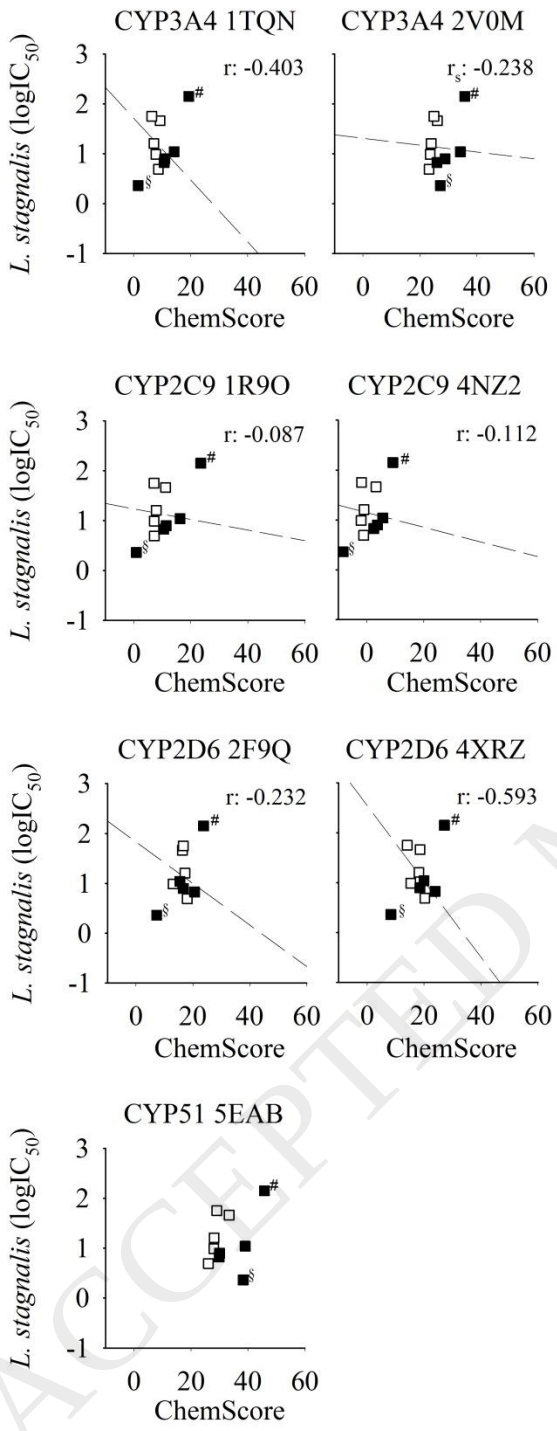

Figure 4. Correlations between inhibition strengths of triazole fungicides (white symbols) and imidazole fungicides (black symbols) toward *L. stagnalis* (n = 8) ECOD activity (in $\log IC_{50}$ μM) and docking scores obtained with constrained docking into human CYP2C9, CYP2D6 and

CYP3A4 and fungal CYP51. "r" and "r_{sp}" denote Pearson or Spearman correlation coefficients, respectively. * denotes a statistically significant correlation. Clotrimazole (§) and ketoconazole (#) were not included in the correlation analysis.

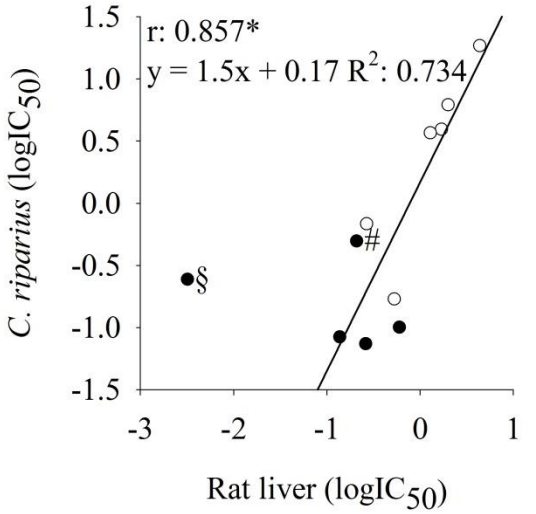

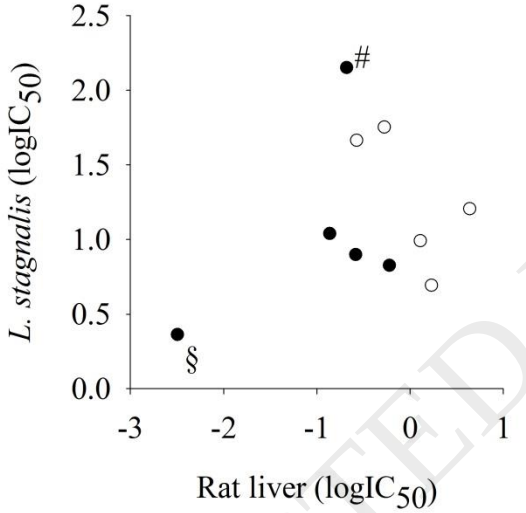

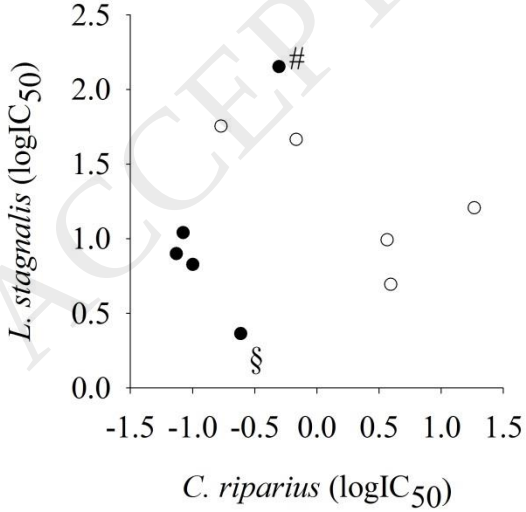

Figure 5. Comparison between inhibition strengths of azole fungicides (imidazoles are shown by black circles and triazoles by white circles) in rat liver, *C. riparius* and *L. stagnalis*, estimated as half maximal inhibition concentrations of cytochrome P450 ECOD activity (in $\log IC_{50}$ μM). Clotrimazole (§) was not included in the correlation and regression analyses, while ketoconazole (#) was included.

Table 1. Azole fungicides used in the present study, type (I: imidazole, T: triazole), use (M: medicine, A: agriculture), CAS number, purity, molecular weight, predicted logP (computed by Chemicalize,[46] based on Viswanadhan, et al. [47]), number of stereoisomers and experimentally measured inhibition strengths toward cytochrome P450 ECOD activity of rat liver, *C. riparius* larvae and *L. stagnalis* (IC_{50} ± SE).

Name	Type	Use	CAS	Purity (%)	Molecular Weight	Predicted logP	Isomers	IC_{50} Rat liver (μM)	IC_{50} *C. riparius* (μM)	IC_{50} *L. stagnalis* (μM)
Bifonazole	I	M	60628-96-8	≥ 98%	310.39	5.23	2	0.14±0.01	0.08±0.01	11±2
Clotrimazole	I	M	23593-75-1	99.6%	344.84	5.84	1	0.0032±0.0008	0.24±0.12	2.3±0.6
Cyproconazole	T	A	94361-06-5	99.6%	291.78	2.85	4	8.4±0.6	n.m.	n.m.
Difenoconazole	T	A	119446-68-3	97.2%	406.26	4.86	4	0.27±0.03	0.68±0.05	46±14
Epoxiconazole	T	A	135319-73-2	99.0%	329.76	3.74	4	2.0±0.2	6.2±0.3	n.m.
Fenbuconazole	T	A	114369-43-6	99.6%	336.82	4.35	2	3.0±0.3	n.m.	n.m.
Fluconazole	T	M	86386-73-4	≥ 98%	306.27	0.56	1	26±4	n.m.	n.m.
Flusilazole	T	A	85509-19-9	99.8%	315.39	4.68	1	0.53±0.07	0.17±0.04	57±12
Imazalil	I	M	58594-72-2	≥ 98%	297.18	3.76	2	0.6±0.2	0.10±0.01	7±1
Ketoconazole	I	M	65277-42-1	≥ 98%	531.43	4.19	4	0.21±0.04	0.50±0.08	142±17
Myclobutanil	T	A	88671-89-0	99.4%	288.78	3.66	2	11±1	n.m.	n.m.
Penconazole	T	A	66246-88-6	≥ 98%	284.18	4.19	2	1.7±0.2	3.9±0.4	4.9±0.5
Prochloraz	I	A	67747-09-5	98.6%	376.67	3.62	1	0.26±0.03	0.074±0.006	8±3
Propiconazole	T	A	60207-90-1	99.1%	342.22	4.33	4	1.29±0.09	3.7±0.2	10±2
Tebuconazole	T	M	107534-96-3	99.3%	307.82	3.69	2	4.4±0.5	18±1	16±2

Tetraconazole	T	A	112281-77-3	99.1%	372.15	3.96	2	4.7±0.3	n.m.	n.m.
Triadimefon	T	A	43121-43-3	99.5%	293.74	3.97	2	16±4	n.m.	n.m.
Triadimenol	T	A	55219-65-3	98.7%	295.76	3.28	4	8±1	n.m.	n.m.